A systematic study of the validation of Oliver and Pharr's method

Siqi Shu, Jian Lu,[a] and Dongfeng Li
Department of Mechanical Engineering, The Hong Kong Polytechnic University, Kowloon, Hong Kong, China

(Received 25 April 2007; accepted 10 August 2007)

Oliver and Pharr's method (O&P's method) is an efficient and popular way of measuring the hardness and Young's modulus of many classes of solid materials. However, there exists a range of errors between the real values and the calculated values when O&P's method is applied to materials not included in the basic assumption proposed initially. In this article, the dimensional analysis theorem and the finite element method are applied to evaluate errors for high elastic ($E/\sigma_Y \rightarrow 5$) to full plastic ($E/\sigma_Y \rightarrow 1000$) materials with different strain-hardening exponents from 0 to 0.5. A new method is proposed to correct errors obtained using O&P's method. The numerical simulation results show that the errors obtained using O&P's method, given in the form of charts, are mainly dependent on the ratio of the reduced Young's modulus to the yield stress (i.e., E_r/σ_Y) and the strain-hardening exponent, n, for an indenter with a fixed included angle. The two mechanical properties, which can be extracted from the load–depth curves of two indenters with different included angles, are used to correct the errors in the hardness and Young's modulus of the indented materials produced by O&P's method.

I. INTRODUCTION

Indentation experiments have been used to measure the hardness of materials for over a century and more during the last 30 years. With the increasing sophistication of indentation equipments, nanoindentation experiments can provide accurate measurements of the continuous variation in the indentation depth P down to the micronanometer level, as a function of the indentation depth h down to nanometer level. The load P versus depth h curves obtained from nanoindentation are like "thumbprints" of the indented materials. They record the elastic and plastic characteristics of indented materials and can be used to investigate their mechanical behaviors and deformation mechanisms. As a result, indentation experiments, with their associated comprehensive theoretical and computational models, have been conducted by numerous researchers on different classes of materials to determine the hardness and other mechanical properties of indented materials.

Measuring hardness using indentation may date back to the work of Tabor[1] and Johnson.[2] Using an energy-based approach, Cheng and Cheng[3–6] presented the relationships among the hardness, the Young's modulus, the irreversible work, and the total work. Cao et al.[7] developed an energy-based method for calculating hardness and Young's modulus within reasonable theoretical error bounds.

Based on Sneddon's solution, Doerner and Nix[8] published a new method with which the hardness can be obtained from the maximum applied load, the contact depth, which is calculated from the maximum indentation depth, and the slope of the initial part of the unloading curve on the assumption that the unloading response is linear.

At present, the most popular method for analyzing hardness and Young's modulus has been proposed by Oliver and Pharr,[9] who expanded on ideas developed by Loubet et al.[10] and Doerner and Nix.[8] Its attractiveness stems largely from the fact that the mechanical properties of the indented materials can be determined by analyzing the load–depth curves obtained from indentation data without needing to visualize the hardness impression. Although Oliver and Pharr[9] indicated that their method may overestimate the hardness and Young's modulus, sometimes by as much as 50%,[11,12] their method has been used to measure the hardness and Young's modulus of many classes of materials, including metals, ceramics, polymers, composites, superhard materials, and even biomaterials. Recently, the method has also been used for anisotropic materials and coatings.[13] According to isiknowledge (ISI) web,[14] the work of Oliver and Pharr,[9]

[a]Address all correspondence to this author.
e-mail: Jian.Lu@inet.polyu.edu.hk
DOI: 10.1557/JMR.2007.0428

 © 2007 Materials Research Society

CAMBRIDGE JOURNALS
http://journals.cambridge.org Downloaded: 04 Oct 2013 IP address: 158.132.161.103

which has been cited more than 3000 times, has been used to calculate the hardness and Young's modulus of many classes of materials (Table I). The method has even been adopted as a standard method and incorporated into high-resolution testing equipments used to measure the hardness and Young's modulus of different classes of materials. However, many authors have argued against the validity of this method because there is no ideal theory that can treat all real cases.[3–6,15–17]

According to Oliver and Pharr[11] and Boshakov and Pharr,[12] pileup of the indented materials around the contact impression, which is affected by the ratio of the reduced Young's modulus to the yield stress and the strain-hardening exponent of the indented materials, is the key to the errors in the hardness and the Young's modulus obtained using Oliver and Pharr's method (O&P's method). For elastic–perfectly plastic materials indented by a rigid cone with a half-included angle of 70.3°, pileup is not obvious when the ratio of the reduced Young's modulus to the yield stress is no more than 89, while for linear-hardening materials with a work-hardening rate of $\eta = d\sigma/d\epsilon = 10$, the above limitation of E_r/σ_Y is about 178. According to the database proposed by Ashby,[18] there are still many materials for which the hardness and Young's modulus cannot be calculated correctly using O&P's method.

Although Oliver and Pharr, and their colleagues have made several important changes to the method that both improve its accuracy and extend its field of application,[11] Ma et al.[15] maintain that the method cannot be used to correctly estimate the hardness and Young's modulus of the indented materials in certain cases. Recently, the sonic methods and atomic force microscopy (AFM) methods have been used to improve O&P's method. However, the sonic methods are limited to improve O&P's method because the tests require the samples to be electrically conductive.[16] And AFM cannot precisely measure the contact area during indentation processing.[17] Furthermore, both methods introduce some new experimental techniques that still need improvements for general applications. It is therefore very important to systematically investigate O&P's method and extend the application of the basic method to a much wider range of materials.

TABLE I. Number of citations (from ISI web).

	Citations (approx.)	Material classes
1	400	Metals
2	500	Ceramics
3	200	Polymers
4	550	Composites
5	200	Biomaterials
6	250	Superhard materials (carbon and nitrogen materials)

For the purposes of clarity, a brief review of O&P's method as it was originally developed is given in Sec. II. Section III gives a detailed description of dimensional analysis and the finite element method for simulating the indentation process. Section IV describes the results obtained using finite element analysis, and gives a new method for calculating the hardness and Young's modulus of indented materials. Section V summarizes the main findings of the present work.

II. A REVIEW OF O&P'S METHOD

O&P's method was proposed to measure the hardness and Young's modulus of elastic–plastic materials according to the load–depth data for one loading–unloading cycle. A typical indentation curve obtained with a conical indenter is presented in Fig. 1. The deformation geometries of the indenter and the indented materials during the unloading process are shown in Fig. 2.

According to the model, the reduced Young's modulus, E_r^{OP}, and the hardness, H_{OP}, of the indented materials can be obtained with O & P's method using the following formulas:

$$H_{OP} = \frac{P_{max}}{A(h_c)} \quad , \tag{1}$$

$$E_r^{OP} = \frac{\sqrt{\pi}}{2\beta} \frac{S}{\sqrt{A(h_c)}} \quad , \tag{2}$$

where P_{max} is the maximum load, $A(h_c)$, h_c, and S represent the maximum contact area, the contact depth, and the initial unloading stiffness at h_{max}, respectively, and β is a correction factor used to take into account the deviations caused by different physical processes. The Young's modulus of indented materials can be calculated using the reduced Young's modulus and the following formula:

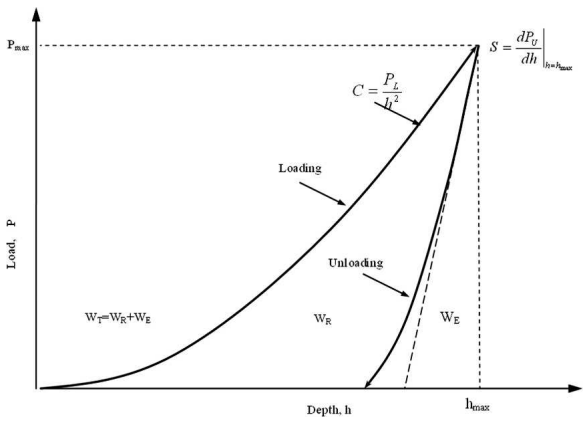

FIG. 1. Schematic illustration of the indentation load–depth data of elastic–plastic materials indented by a sharp indenter.

CAMBRIDGE JOURNALS
http://journals.cambridge.org Downloaded: 04 Oct 2013 IP address: 158.132.161.103

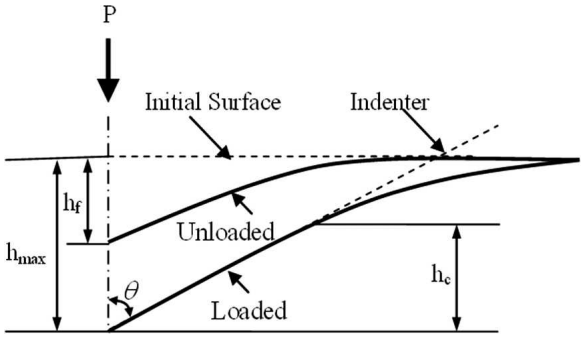

FIG. 2. Schematic illustration of the contact geometry during the unloading process.

$$\frac{1}{E_r} = \frac{1-\nu^2}{E} + \frac{1-\nu_i^2}{E_i} \quad , \tag{3}$$

where E and ν are the Young's modulus and Poisson ratio of the indented materials, respectively, and E_i and ν_i are the Young's modulus and Poisson ratio of the indenter, respectively.

To calculate the Young's modulus and hardness of the indented materials accurately, Oliver and Pharr made some initial suppositions.[9,11]

First, it is assumed that elastic–plastic deformation occurs during loading, but that elastic deformation only occurs during unloading. Unlike the method proposed by Doerner and Nix,[8] O&P's method assumes that the unloading curves are distinctly curved instead of linear, and are usually approximated well by the power-law relationship:

$$P = \alpha(h - h_f)^m \quad , \tag{4}$$

where α and m are power-law-fitting constants and the variation of the power-law exponents is in the range of $1.2 \leqslant m \leqslant 1.6$, which shows that a flat punch approximation is inadequate because $m = 1$ in the method proposed by Doerner and Nix.[8] The unloading slope at maximum depth can be calculated using the following formula:

$$S = \left.\frac{dP}{dh}\right|_{h=h_{max}} \quad . \tag{5}$$

Second, according to the same depth-to-area relationship, it is assumed that a pyramid indenter can be modeled by a conical indenter with a half-included angle, θ.

Third, the assumption is that the contact periphery sinks in a way that can be described by models for the indentation of a flat elastic half-space by rigid punches of simple geometry. In this case, the contact depth is given by

$$h_c = h_{max} - \epsilon \frac{P_{max}}{S} \quad , \tag{6}$$

where ϵ is a constant that depends on the geometry of the indenter. The corresponding value is 0.72 for a conical indenter, 0.75 for an indenter with a parabola of revolution, and 1 for a flat punch.

Fourth, the indenter is often considered to be rigid, and the reduced Young's modulus is introduced into the model to reduce the effect of elastic deformation of the indenter in Eq. (3). However, as yet, its rationality has not been proven theoretically. This assumption can reduce the effect of the elastic deformation of the indenter on the measured values of hardness and Young's modulus when the Young's modulus of the indented materials is lower than that of the indenter. However, this will need to be tested if the Young's modulus of the indented materials is close to that of the indenter.

Finally, the correction factor β in Eq. (2) plays a very important role in reducing the discrepancy between the real value and the calculated value caused by various physical processes. King[19] was the first to study the importance of correction and found that $\beta = 1.034$ for a triangular indenter and $\beta = 1.012$ for a square-based indenter. Vlassak and Nix[20] later found that $\beta = 1.058$ for a flat-ended punch. By studying Sneddon's original solution, Hay et al.[21] found that it was necessary to provide a correction factor and found the $\beta = 1.067$ for materials with a Poisson ratio of $\nu = 0.3$ and an indenter with a half-included angle of 70.3°. Oliver and Pharr[11] proposed that β should lie within a range of $1.0266 \sim 1.085$ and that $\beta = 1.05$ is as good a choice as any. However, Cao et al.[22] proposed that the correction factor might be affected by the Poisson's ratio and the ratio of the Young's modulus of the indenter to the Young's modulus of the indented materials.

Based on the above assumptions, O&P's method can be used to correctly calculate the hardness and Young's modulus of the most common materials. The question arises as to whether or not it can be used to correctly measure other materials. The purpose of this study is to evaluate the effectiveness of O&P's method and to propose a new method to correct it.

III. DIMENSIONAL ANALYSIS AND COMPUTATIONAL MODEL

A. Dimensional analysis

The mechanical behavior of solid materials is often described as homogeneous elastic–plastic deformation. When they are less than the initial yield stress, materials are linear elastic and after yielding, the stress–strain curves of the materials are assumed to have the power-law hardening shown in Fig. 3. The relationships can be described as follows:

$$\sigma = \begin{cases} E\epsilon & , \quad \sigma \leq \sigma_Y \\ \sigma_Y(\epsilon/\epsilon_Y)^n, & \sigma > \sigma_Y \end{cases} \quad . \tag{7}$$

CAMBRIDGE JOURNALS
http://journals.cambridge.org Downloaded: 04 Oct 2013 IP address: 158.132.161.103

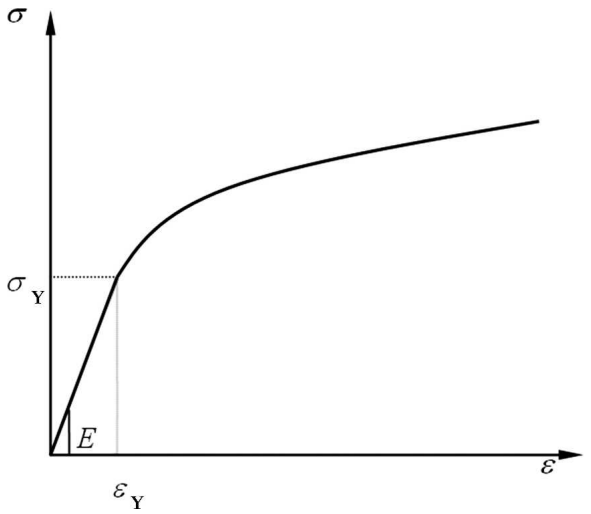

FIG. 3. Schematic illustration of the power-law stress–strain relationship.

The indented materials can therefore be characterized by the Young's modulus, E, the Poisson's ratio, ν, the initial yield stress, σ_Y and the strain-hardening exponent, n. The indenter deforms elastically during indenting, and so it can be characterized by the Young's modulus, E_i, and Poisson's ratio, ν_i.

Dimensional analysis has often been used to study indentation problems in recent years.[3–6,23,24] In the present study, dimensional analysis is still used to study the effects of the hardness and the Young's modulus of indented materials and to further evaluate the effectiveness of O&P's method.

For a sharp indenter that indents a power-law elastic–plastic solid in the usual way, the indenter can be characterized by a half-included angle, θ. The friction coefficient at the contact surface between the indenter and the indented material can be assumed to be zero.[25] Thus, during loading, the force P on the indenter can be written as

$$P = f_0(E_i,\nu_i;\ E,\sigma_Y,n,\nu;\ \theta;\ h) \quad . \tag{8}$$

According to Dao et al.[26]:

$$P = f_1(E_r,\sigma_Y,n;\ \theta;\ h) \quad . \tag{9}$$

By applying the Π theorem of dimensional analysis, the true hardness of indented materials can be described using the following dimensionless expression:

$$\frac{H}{\sigma_Y} = \Pi_1\left(\frac{E_r}{\sigma_Y},\ n,\ \theta\right) \quad . \tag{10}$$

The hardness and the Young's modulus obtained using O&P's method can be expressed by the following dimensionless expressions using Eqs. (1) and (2):

$$\frac{H_{OP}}{\sigma_Y} = \Pi_2\left(\frac{E_r}{\sigma_Y},\ n,\ \theta\right) \quad , \tag{11}$$

$$\frac{E_r^{OP}}{E_r} = \Pi_3\left(\frac{E_r}{\sigma_Y},\ n,\ \theta\right) \quad . \tag{12}$$

Furthermore, the relative errors in the hardness and Young's modulus obtained using O&P's method can be derived using Eqs. (10)–(12):

$$\frac{H_{OP}-H}{H} = \Pi_4\left(\frac{E_r}{\sigma_Y},\ n,\ \theta\right) \quad , \tag{13a}$$

$$\frac{E_r^{OP}-E_r}{E_r} = \Pi_5\left(\frac{E_r}{\sigma_Y},\ n,\ \theta\right) \quad . \tag{13b}$$

Therefore, the fundamental material properties affecting the hardness and the Young's modulus are the ratio of the reduced modulus to the yield stress, E_r/σ_Y, and the strain-hardening exponent, n, for an indenter with a fixed included angle.

It has been demonstrated that only two independent parameters can be determined from a single load–depth curve.[27,28] In the present study, the indentation loading curvature C and the ratio of the residual work to the total work done by the indenter W_R/W_T are adopted without losing generality. According to the work of Tho et al.,[23] the mechanical parameters of the indented materials can be determined with loading curvature and work from two indenters with various included angles. Dimensionless relationships therefore exist between the mechanical parameters and the loading curvatures as well as the work done by the indenter as follows:

$$\frac{C_{\theta_1}}{C_{\theta_2}} = \Pi_6\left(\frac{E_r}{\sigma_Y},\ n\right) \quad , \tag{14}$$

$$\frac{\left.\frac{W_R}{W_T}\right|_{\theta_1}}{\left.\frac{W_R}{W_T}\right|_{\theta_2}} = \Pi_7\left(\frac{E_r}{\sigma_Y},\ n\right) \quad . \tag{15}$$

B. Computational model

According to the same depth-to-area relationships, a pyramid indenter is equivalent to a conical indenter. For example, the equivalent angle of a Berkovich indenter is 70.3°.[29] The indentations of a conical indenter are shown schematically in Fig. 4. The materials around the indenter usually pile up or sink in during indenting of the indenter.

Finite element calculations using ABAQUS[30] have been carried out to simulate the indentation in the work of Cheng and Cheng,[3–6] Dao et al.,[26] and Jayaraman et al.[31] In their work, the indenter was considered as a rigid

CAMBRIDGE JOURNALS
http://journals.cambridge.org Downloaded: 04 Oct 2013 IP address: 158.132.161.103

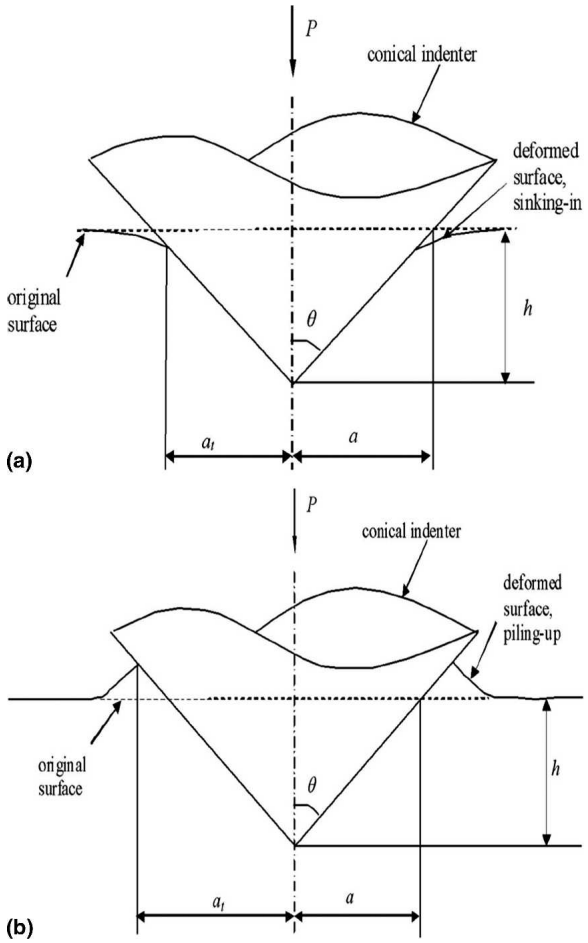

FIG. 4. Schematic illustration of a conical indenter's indentation: (a) sink-in; and (b) pileup.

body and the indented materials were modeled as elastic–plastic solids. In the present research, an axisymmetric two-dimensional finite element model is constructed to simulate the indentation procedure of an elastic indenter indenting elastic–plastic materials. The finite element computations in this section are also carried out using ABAQUS[30] for different combinations of dimensionless values: E_r/σ_Y, n, and θ. In the simulations, the Von Mises yield criterion is used. Figure 5 shows the mesh design for axisymmetric calculation. A total of 415 and 12,000 four-node bilinear axisymmetric elements, respectively, are used for the indenter and the indented materials. The mesh has been tested for convergence and determined to be insensitive to far-field boundary conditions. Friction has a negligible impact on the present numerical simulations.[25]

The boundary conditions on the indented solid are such that the lowest surface is fixed in all directions and the left surface of the indented materials and the indenter is fixed in the direction r. The boundary has negligible effects on the computational value because the boundary is at a sufficient distance from the indented point on the indented materials. Figure 6 is a schematic illustration of the boundary conditions. In the simulation, a rigid indenter rod has been used. The upper surface of the indenter has a finite displacement in the direction z that is the same as that of the indenter rod. There is no displacement in the direction r.

To compare the numerical results from the previous finite element model of the rigid indenter with that from the present model, the indentations of the material with the mechanical properties of $E = 200$ GPa, $\sigma_y = 2$ GPa, $n = 0.3$, and $v = 0.3$ are simulated in Fig. 7. The calculation results using the present model agree well with those from the previous finite element model when the ratio of Young's modulus of the indenter to that of the indented materials is large (e.g., $E_i/E = 50$). And the smaller the ratio of the Young's modulus of the indenter to that of the indented materials is, the larger is the discrepancy of the numerical results from the two models. To further test the validity of the present finite element model, the experimental stress–strain data of 7075-T651 aluminum from the work of Dao et al.[26] were used as inputs for the numerical simulations. The indenter is defined as $E_i = 1140$ GPa and $v_i = 0.07$. The indentation responses from the experiments and numerical simulations are shown in Fig. 8, respectively. And it shows that

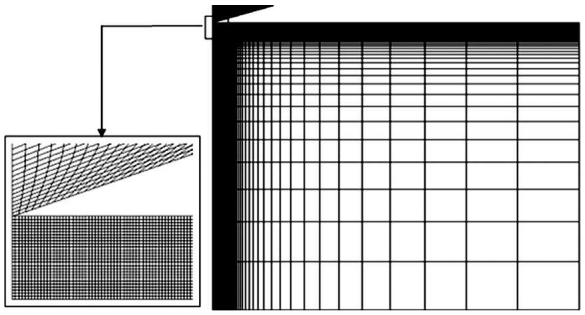

FIG. 5. Schematic illustration of finite element mesh.

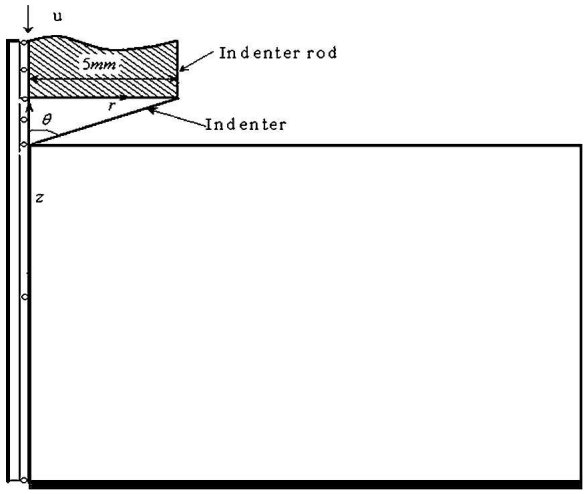

FIG. 6. Boundary conditions of numerical simulation.

CAMBRIDGE JOURNALS
http://journals.cambridge.org Downloaded: 04 Oct 2013 IP address: 158.132.161.103

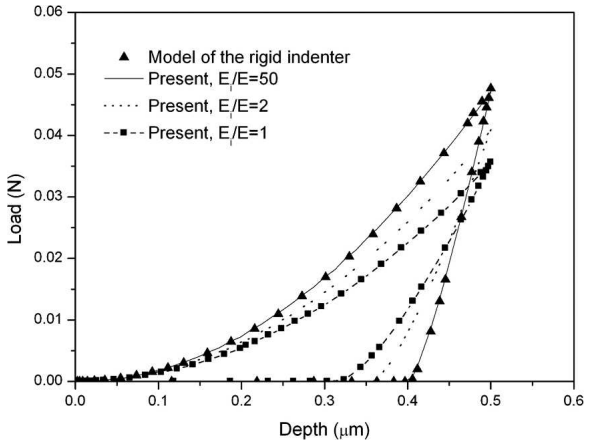

FIG. 7. Indentation curves obtained from two finite element models for indented materials with mechanical properties of $E = 200$ GPa, $\sigma_Y = 2$ GPa, $n = 0.3$, and $v = 0.3$.

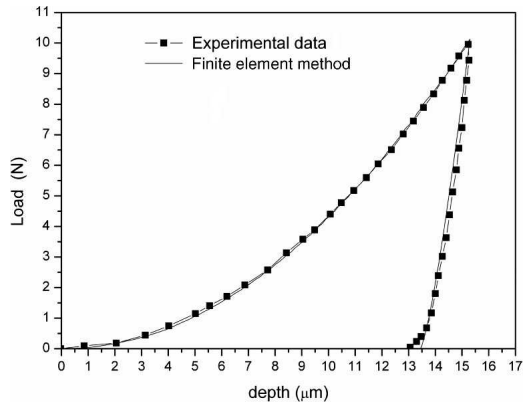

FIG. 8. Comparison between experimental and computational responses of 7075-T651 aluminum.

the computational P–h curve corresponds well to the experimental curve, although some errors, which can be considered negligible, exist. The finite element model can therefore be used to simulate the indenting test.

IV. COMPUTATIONAL RESULTS

According to Eqs. (10)–(13), the dimensionless parameters, H/σ_Y, H_{OP}/σ_Y, $(H_{OP} - H)/H$, and $(E_r^{OP} - E_r)/E_r$ are dependent on E_r/σ_Y, n, and θ, respectively. However, because there are no analytical solutions to the problem of an elastic conical indenter in relation to elastic–plastic-indented materials, we chose to use the finite element method to evaluate the dimensionless function, Π_1, Π_2, Π_4, and Π_5. To cover a large range of materials from purely elastic to full plastic, the values of E_r/σ_Y are in the range of 5 ~ 10,000, and the strain-hardening exponents, n, vary from 0 to 0.5. The Poisson ratios, v_i and v, of the indenter and the indented materials, respectively, are fixed at 0.07 and 0.3, respectively, because the effect of the Poisson ratios on the calculated hardness and Young's modulus is not marked.

The discrepancy between the real values and the calculated values of the hardness and Young's modulus obtained using O&P's method will be discussed in the following sections.

A. The effect of E_r/σ_Y and n on the hardness and Young's modulus of the indented materials

The results of the finite element studies in Figs. 9 and 10 show to what extent $(H_{OP} - H)/H$ and $(E_r^{OP} - E_r)/E_r$ depend on E_r/σ_Y and n, which converge on a master curve for a wide variety of materials with different E_r/σ_Y ratios and a fixed n when Berkovich indenter is used.

According to Fig. 9, O&P's method can be used to calculate the hardness of the materials, of which the strain-hardening exponent is about 0.3 with small errors. The method usually overestimates the hardness of materials with little or no capacity for work hardening, and underestimates the hardness of materials with a higher capacity for work hardening (e.g., $n = 0.5$). The errors produced by O&P's method increase steadily as E_r/σ_Y increases for materials with given strain-hardening exponents.

The results in Fig. 10 show that the errors in the Young's modulus obtained using O&P's method depend on E_r/σ_Y and n. The Young's modulus of materials with strain-hardening exponents equal to 0.5 can be calculated correctly using O&P's method. However, for materials with a lower n, the errors in the Young's modulus produced using O&P's method are greater. The higher the values for E_r/σ_Y, the larger the errors of Young's modulus will be for materials with the same strain-hardening exponents.

To study the field of application of O&P's method, the database proposed by Ashby et al.[32] has been adopted in conjunction with numerical results. It can be seen in Figs. 11(a) and 11(b) that the calculations made with the finite element method in the shaded area cover most engineering materials. It is assumed that O&P's method is valid when the relative errors in the hardness and Young's

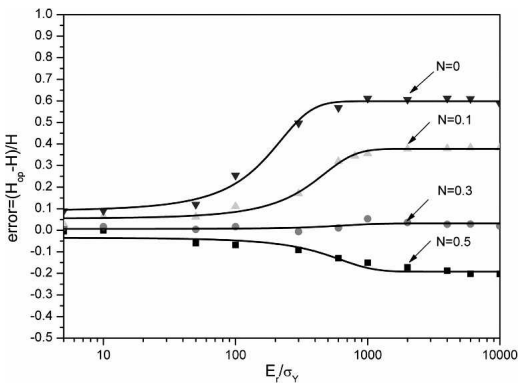

FIG. 9. The relative errors of the hardness from O&P's method.

CAMBRIDGE JOURNALS
http://journals.cambridge.org Downloaded: 04 Oct 2013 IP address: 158.132.161.103

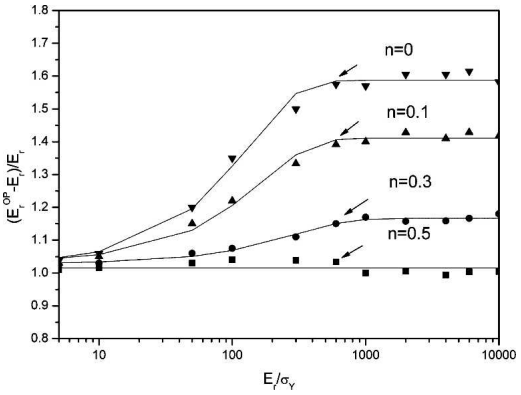

FIG. 10. The relative errors of the Young's modulus from O&P's method.

modulus obtained are below 10%. The hardness and the Young's modulus of materials with different strain-hardening exponents, which are in the zone between the two corresponding lines in the shaded area in Figs. 11(a) and 11(b), can be calculated correctly using O&P's method.

Figure 11(a) can be used to correctly calculate the hardness of all ceramics, composites, metals, and polymers with a strain-hardening exponent equal to 0.3 in the shaded area using O&P's method. However, many materials exist that have a higher strain-hardening exponent (e.g., $n = 0.5$), the hardness of which is underestimated, and a large number of materials have a lower strain-hardening exponent (e.g., $n = 0$ and 0.1), the hardness of which is overestimated. Figure 11(b) can be used to correctly calculate the Young's modulus of all ceramics, composites, metals, and polymers with a strain-hardening exponent of 0.5 in the shaded area, using O&P's method. However, a large number of materials exist that have a lower strain-hardening exponent (e.g., $n = 0$, 0.1, and 0.3), the Young's modulus of which is overestimated. Therefore, a large number of ceramics, composites, metals, and polymers in Figs. 11(a) and 11(b) exist, the hardness and Young's modulus of which cannot be calculated correctly.

In the present study, the indented materials are described as elastic–plastic materials, and the uniaxial stress–strain relationships of the indented materials are given in Eq. (7). However, the uniaxial stress–strain curves of polymers are often brittle, or nonlinearly elastic. Additional attention is therefore needed when Figs. 11(a) and 11(b) are used for polymers. Also, cracks often occur when indenting ceramics. As a result, Figs. 11(a) and 11(b) are valid only when the cracks have a negligible effect on the elastic–plastic deformation of the ceramics.

It should be especially noted that errors exist when sink-in occurs in the case of indented materials with a higher strain-hardening exponent, such as those materials with a strain-hardening exponent equal to 0.5 in Fig. 9. Therefore, sink-in is not the best way to judge whether hardness can be calculated accurately using O&P's method. It may be caused by the constant value of the correction factor β.

B. Determination of parameters E_r/σ_Y and n

It has been proved that the mechanical properties of indented materials could not be determined by using the load–depth curve from a single sharp indenter according to the work of Cheng and Cheng,[33] Capehart and Cheng,[34] Tho et al.,[27] and Alkorta et al.[28] So spherical indenter-based inverse analysis[35] and different dual-indenter inverse analyses have been developed to determine the mechanical properties of indented materials. Based on the representative stress, the dual-indenter reverse analyses proposed by Bucaille et al.[36] and Chollacoop et al.[37] could be used to determine the mechanical properties of a certain range of materials. Cao et al.[38] developed an energy-based method to extract plastic properties of metal materials, but the Young's modulus must be known in advance. The artificial neural network must be mastered and training patterns must be owned, although Young's modulus, yield stress, and stain-hardening exponents can be obtained by using the inverse analysis proposed by Tho et al.[27] In the present article, the mechanical properties (E_r, σ_Y, and n) may be obtained by using a simplified approach.

In the present article, based on the loading curvature and the work done by the indenters, a dual-indenter inverse analysis for a large range of materials is developed to determine the parameters of E_r/σ_Y and n, which are the critical values that affect the measurement of the hardness and Young's modulus according to the analysis described in the subsection above. The relationships between these two parameters and $C_{\theta_1}/C_{\theta_2}$, as well as $\left.\frac{W_R}{W_T}\right|_{\theta_1} \Big/ \left.\frac{W_R}{W_T}\right|_{\theta_2}$ are shown in Eqs. (14) and (15), which, depending on the numerical results, can be expressed as the following polynomials:

$$\ln\left(\frac{E_r}{\sigma_Y}\right) = \frac{a_0}{1+e^{-(a_1\Omega+a_2\Psi+a_3)}} + \frac{a_4}{1+e^{-(a_5\Omega+a_6\Psi+a_7)}} + \frac{a_8}{1+e^{-(a_9\Omega+a_{10}\Psi+a_{11})}} + a_{12} \quad , \tag{16}$$

$$n = \frac{b_0}{1+e^{-(b_1\Omega+b_2\Psi+b_3)}} + \frac{b_4}{1+e^{-(b_5\Omega+b_6\Psi+b_7)}} + \frac{b_8}{1+e^{-(b_9\Omega+b_{10}\Psi+b_{11})}} + b_{12} \quad , \tag{17}$$

CAMBRIDGE JOURNALS
http://journals.cambridge.org Downloaded: 04 Oct 2013 IP address: 158.132.161.103

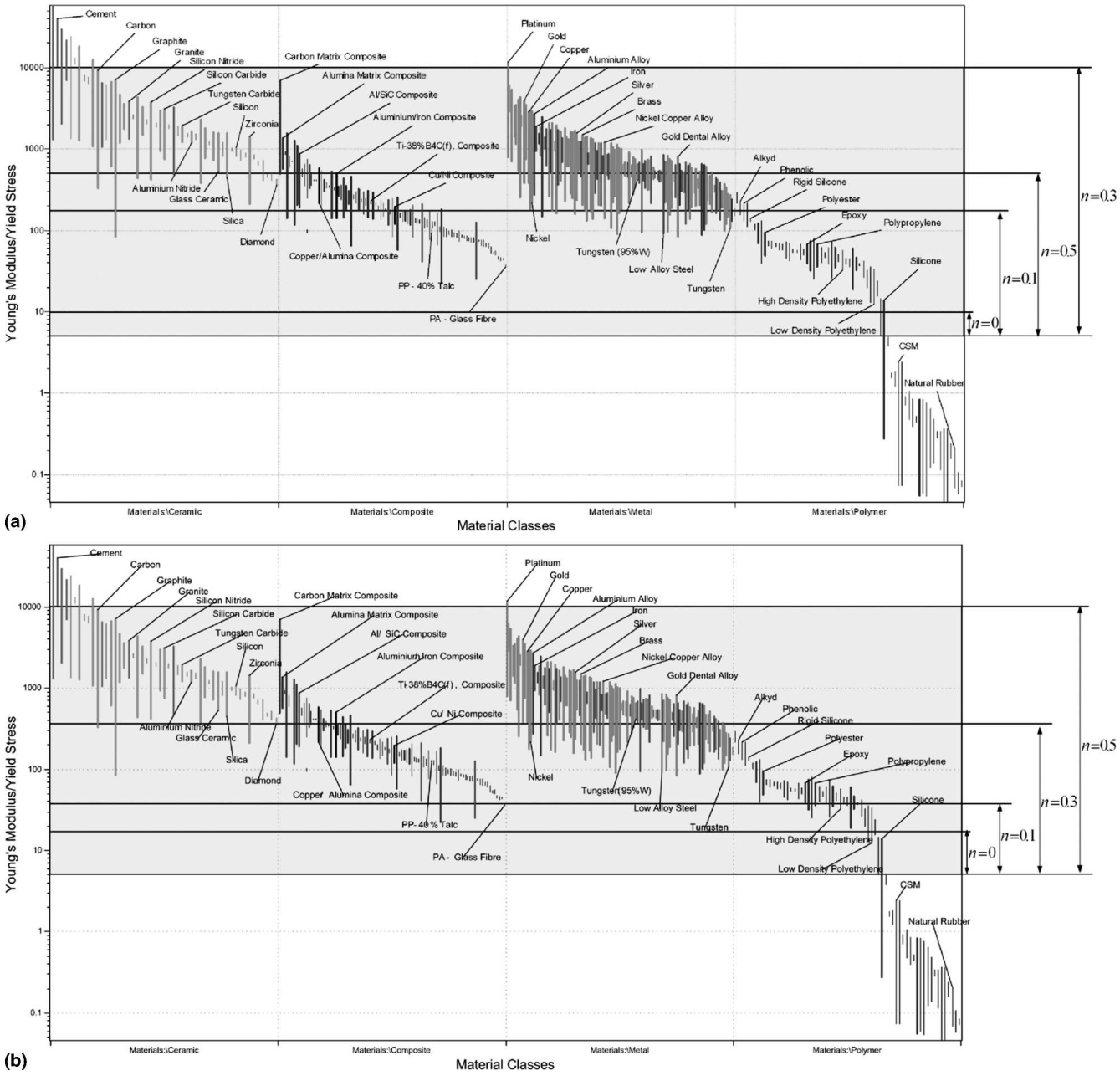

FIG. 11. The different classes of materials with different values of n, from which the hardness and Young's modulus can be calculated correctly using O&P's method with Berkovich indenter, are shown by arrows pointing outward: (a) hardness; and (b) Young's modulus.

where,

$$\Psi = \frac{C_{\theta_1}}{C_{\theta_2}} \quad , \tag{18}$$

$$\Omega = \frac{\left.\frac{W_R}{W_T}\right|_{\theta_1}}{\left.\frac{W_R}{W_T}\right|_{\theta_2}} \quad . \tag{19}$$

The two best-fit functions with the root mean square errors of 0.2% and 0.012% are obtained using Eqs. (16) and (17), respectively. And the coefficients in the two equations are given in Table II when $\theta_1 = 80°$ and $\theta_2 = 50°$. The existence, uniqueness, and sensitivity of the solutions to the inverse problem have been discussed in detail in another recent work of our team.[39] Furthermore, based on experimental results, the parameters E_r/σ_Y and n, can be obtained from the loading curvatures and the ratios of the residual work to the total work from indentation.

CAMBRIDGE JOURNALS
http://journals.cambridge.org Downloaded: 04 Oct 2013 IP address: 158.132.161.103

TABLE II. Coefficients in Eqs. (16) and (17).

	Coefficients				
Eq. (16)	a0 = 1412.86136	a1 = 2.39979	a2 = −0.36134	a3 = −1.82881	a4 = 4113.83424
	a5 = −2.14182	a6 = 0.3539	a7 = 2.80139	a8 = 3049.35672	a9 = 16.44837
	a10 = −0.00558	a11 = −22.7925	a12 = −4109.49625		
Eq. (17)	b0 = 0.37508	b1 = 40.7477	b2 = 7.00538	b3 = −82.62004	b4 = 584.64567
	b5 = −2.1818	b6 = −0.12384	b7 = −3.57708	b8 = −4.85045	b9 = −5.46432
	b10 = 0.01752	b11 = 2.3074	b12 = −0.09362		

It is well known that real indentation measurements are influenced by the tip rounding of the indenter and the compliance of the machine. However, in the present method the effect of tip rounding of the indenter could be drastically reduced by enlarging the indentation depth. In this case, the ratio of indentation depth to tip radius of the indenter should be >10 according to our numerical simulations. To eliminate the effect of the compliance of machine the measured indentation load–depth curves must be modified with the compliance values of machine, γ, which are in the range of 2–6 nm/mN for the Hysitron TriboIndenter (Hysitron Inc., Minneapolis, MN).[40]

C. A new correction for O&P's method

According to the above analysis, the real hardness and the Young's modulus of the indented materials can be obtained using Figs. 9 and 10 together with the values of E_r/σ_Y and n, which are described in detail below:

(i) For materials with known mechanical properties, E_r/σ_Y and n, go directly to step 3.

(ii) Carry out indentation experiments using two indenters with different half-included angles (e.g., $\theta_1 = 80°$, and $\theta_2 = 50°$) and obtain two indentation responses. The loading curvatures and the ratio of the residual work to the total work can be obtained from the two indentation responses. E_r/σ_Y and n can be obtained from Eqs. (16) and (17).

(iii) The relative errors in the hardness and Young's modulus (e_H and e_E) can be obtained using the values of E_r/σ_Y and n in conjunction with Figs. 9 and 10.

(iv) Based on the indentation response from the 80° indenter, the hardness and Young's modulus obtained using O&P's method can be corrected using the

TABLE III. The exact, identified mechanical properties of eight materials.

Materials	E (GPa) (true)	E/σ_Y (true)	n (true)	H (MPa) (true)	E_r/σ_Y (identified)	n (identified)	H (MPa) (O&P's method)
Copper[a]	120	1714	0.5	2295	1465	0.50	1956
Ni[a]	214	1070	0.15	1088	1057	0.15	1379
Steel[b]	210	538	0	1010	400	0.01	1570
Alumina[c]	350	80	0	11,500	65	0	13,880
CNT–Cu[d]	150	882	0.064	601	1197	0.07	861
Carbon–Al[e]	56	161	0.075	1122	191	0.08	1402
Ti–6Al–4V[f]	147	461	0.5	5321	365	0.51	4681
Polyamide[g]	1.56	47	0.004	88	59	0.01	97

Materials	e_H (%) (estimated)	H (MPa) (identified)	Error (%) (hardness)	E (GPa) (O&P's method)	e_E (%) (estimated)	E (GPa) (identified)	Error (%) (Young's modulus)
Copper[a]	−19	***2425***	***5.6***	127.7	2	***125***	***4.2***
Ni[a]	25	***1103***	***1.4***	286	25	***229***	***6.9***
Steel[b]	50	***1050***	***4***	331	55	***213***	***1.5***
Alumina[c]	15	***12,070***	***4.7***	454	25	***363***	***3.7***
CNT–Cu[d]	50	***573***	***−4.6***	214	45	***147***	***2***
Carbon–Al[e]	19	***1178***	***5***	74	27	***58***	***3.6***
Ti–6Al–4V[f]	−13	***5380***	***1.1***	152	2	***150***	***1***
Polyamide[g]	13	***86***	***−2.3***	1.79	18	***1.52***	***2.6***

[a]Taken from Table IV in the work of Cao et al.[38]
[b]Taken from Table 1 in the work of Fisher-Cripps and Brian.[41]
[c]Taken from Fig. 6 (25°) in the work of Estibaliz et al.[42]
[d]Taken from Fig. 4a (5%) in the work of Kim et al.[43]
[e]Taken from Fig. 2 in the work of Zhou et al.[44]
[f]Taken from Fig. 4b in the work of Boehlert et al.[45]
[g]Taken from Fig. 2 (0.4%/min) in the work of Rupnowski et al.[46]

CAMBRIDGE JOURNALS
http://journals.cambridge.org Downloaded: 04 Oct 2013 IP address: 158.132.161.103

corresponding relative errors by means of the following equations:

$$H^1 = \frac{H_{OP}}{1 + e_H} \quad , \tag{20a}$$

$$E_r^1 = \frac{E_r^{OP}}{1 + e_E} \quad , \tag{20b}$$

where,

$$e_H = \frac{H_{OP} - H}{H} \quad , \tag{21}$$

$$e_E = \frac{E_r^{OP} - E_r}{E_r} \quad , \tag{22}$$

(v) The Young's modulus of indented materials can be obtained using the Young's modulus and Poisson's ratio of the indenter according to Eq. (3).

To verify the effectiveness of the method cited above, several materials with different mechanical properties, which have been extracted from stress and strain curves produced by various research teams, are studied with the numerical method shown in Table III.[1–7,38,41–46] The indentation procedures with two indenters, the half-included angles of which were 80° and 50°, respectively, are simulated with the finite element method, and the two indentation responses are obtained. The plastic properties of the indented materials are obtained using Eqs. (16) and (17), which are then used to correct the hardness and Young's modulus errors obtained using O&P's method.

The corrected hardness and the Young's modulus (bold italic type) are compared with the real values in Table III. It can be seen that the hardness and the Young's modulus determined using this method, the relative errors of which are shown to be <10% in Table III (bold italic type), are closer to the real values. This method can therefore be widely used to study the hardness and Young's modulus of indented materials in conjunction with O&P's method.

V. CONCLUSION

In the present study, the effectiveness of O&P's method has been discussed in detail using dimensional analysis and the finite element method, and a new method designed to obtain "true" hardness and "true" Young's modulus for indented materials has been developed. The main contributions and future prospects of this new method are as follows.

The range of errors in the hardness and Young's modulus of indented materials obtained using O&P's method is shown by simulating the indentation of a large number of materials from high elastic ($E/\sigma_Y \rightarrow 5$) to full plastic ($E/\sigma_Y \rightarrow 10{,}000$) with different strain-hardening exponents from 0 to 0.5. Error charts have been drawn up using numerical results. The results show that the hardness of materials with a medium strain-hardening exponent (e.g., $n = 0.3$) can be estimated correctly using O&P's method. However, the method tends to overestimate the hardness of indented materials with a smaller value of n and to underestimate the hardness of indented materials with a larger value of n for a given E_r/σ_Y ratio. The Young's modulus of indented materials with a higher strain-hardening exponent (e.g., $n = 0.5$) can be calculated quite accurately. However, the smaller the strain-hardening exponent is, the higher are the errors obtained using O&P's method for materials with a given E_r/σ_Y. The errors produced by O&P's method increase with the E_r/σ_Y, and can reach about 60% for some materials.

The mechanical properties of indented materials, E_r/σ_Y and n, are the crucial factors that determine the errors produced by O&P's method. They depend on the ratios of the residual work to the total work and on the loading curvature of two loading-depth curves from two different indenters. And the one-to-one-relationships among E_r/σ_Y, n, and $C_{80°}/C_{50°}$, $\left.\frac{W_R}{W_T}\right|_{80°} \Big/ \left.\frac{W_R}{W_T}\right|_{50°}$ have been established.

According to error charts (Figs. 9 and 10) based on numerical simulation and the values of E_r/σ_Y and n obtained using the dual-indenter method, O&P's method has been corrected and a new method has been put forward that can largely reduce the errors. Several classes of materials have been used to prove the validity of this new method.

The database proposed by Ashby[18] and the numerical simulation results have been used to study the field of application of O&P's method. We have demonstrated that the hardness and the Young's modulus of some special materials can be calculated correctly for metals, ceramics, composites, and polymers.

The present method will be further verified by future research experiments, and will be used to calculate the hardness and Young's modulus of indented materials in conjunction with our experiments. In another direction, the included angle of the indenter is also an important parameter that affects the precision of the estimated hardness and Young's modulus. The effects of the indenter angle will also be discussed in our future research.

ACKNOWLEDGMENTS

The authors would like to thank the reviewers for their constructive and helpful comments, acknowledge the financial support of the Hong Kong Polytechnic University funds for niche areas under Grant No. BB90, and the

CAMBRIDGE JOURNALS
http://journals.cambridge.org Downloaded: 04 Oct 2013 IP address: 158.132.161.103

Innovation Technology Commission of the Government of the Hong Kong Special Administrative Region (HKSAR) under Grant No. GHP/043/06.

REFERENCES

1. D. Tabor: *Hardness of Metal* (Clarendon Press, Oxford, 1951).
2. K.L. Johnson: *Contact Mechanics* (Cambridge University Press, Cambridge, 1985).
3. Y.T. Cheng and C.M. Cheng: Scaling relationships in conical indentation of elastic-perfectly plastic solids. *Int. J. Solids Struct.* **36,** 1231 (1997).
4. Y.T. Cheng and C.M. Cheng: Relationships between hardness, elastic modulus, and the work of indentation. *Appl. Phys. Lett.* **73,** 614 (1998).
5. Y.T. Cheng and C.M. Cheng: Scaling relationships in conical indentation of elastic-perfectly plastic solids. *Int. J. Solids Struct.* **36,** 1231 (1998).
6. Y.T. Cheng and C.M. Cheng: Scaling, dimensional analysis, and indentation measurements. *Mater. Sci. Eng., R* **44,** 91 (2004).
7. Y.P. Cao, X.Q. Qian, and J. Lu: On the determination of reduced Young's modulus and hardness of elastoplastic materials using a single sharp indenter. *J. Mater. Res.* **21,** 215 (2006).
8. M.F. Doerner and W.D. Nix: A method for interpreting the data from depth-sensing indentation instruments. *J. Mater. Res.* **1,** 601 (1986).
9. W.C. Oliver and G.M. Pharr: An improved technique for determining hardness and elastic modulus using load and displacement sensing indentation experiments. *J. Mater. Res.* **7,** 1564 (1992).
10. J.L. Loubet, J.M. Georges, O. Marchesini, and G. Meille: Vickers indentation curves of magnesium-oxide (MGO). *Tribology* **106,** 43 (1984).
11. W.C. Oliver and G.M. Pharr: Measurement of hardness and elastic modulus by instrumented indentation: Advances in understanding and refinements to methodology. *J. Mater. Res.* **19,** 3 (2004).
12. A. Bolshakov and G.M. Pharr: Influences of pile up on the measurement of mechanical properties by load and depth-sensing indentation techniques. *J. Mater. Res.* **13,** 1049 (1998).
13. V. Gorokhovsky, C. Bowman, P. Gannon, D. VanVorous, A.A. Voevodin, A. Rutkowski, C. Muratore, R.J. Smith, A. Kayani, D. Gelles, V. Shutthanandan, and B.G. Trusov: Tribological performance of hybrid filtered arc-magnetron coatings, Part 1: Coating deposition process and basic coating basic coating properties characterization. *Surf. Coat. Technol.* **201,** 3732 (2006).
14. ISI: http://portal.isiknowledge.com (2007).
15. D.J. Ma, T.H. Zhang, and C.W. Ong: Evaluation of the effectiveness of representative method for determining Young's modulus and hardness from instrumented indentation data. *J. Mater. Res.* **21,** 225 (2006).
16. C. Aksel and F.L. Riley: Young's modulus measurements of magnesia-spinel composites using load-deflection curves, sonic modulus, strain gauges and Rayleigh waves. *J. Eur. Ceram. Soc.* **23,** 3089 (2003).
17. G. Aldrich-Smith, N.M. Jennett, and U. Hangen: Direct measurement of nanoindentation area function by metrological AFM. *Z. Metallkd.* **96,** 1267 (2005).
18. M.F. Ashby: *Materials Selection in Mechanical Design*, 3rd ed. (Pergamon Press, Oxford, 1985).
19. R.B. King: Elastic analysis of some punch problems for a layered medium. *Int. J. Solids Struct.* **23,** 1657 (1987).
20. J.J. Vlassak and W.D. Nix: Measuring the elastic properties of anisotropic materials by means of indentation experiments. *J. Mech. Phys. Solids* **42,** 1223 (1994).
21. J.C. Hay, A. Bolshakov, and M.M. Pharr: A critical examination of the fundamental relations used in the analysis of nanoindentation data. *J. Mater. Res.* **14,** 2296 (1999).
22. Y.P. Cao, M. Dao, and J. Lu: A precise correction method for the study the superhard materials using the nanoindentation. *J. Mater. Res.* **22,** 1255 (2007).
23. K.K. Tho, S. Swaddiwudhipong, Z.S. Liu, and J. Hua: Artificial neural network model for material characterization by indentation. *Modell. Simul. Mater. Sci. Eng.* **12,** 1055 (2004).
24. Y.G. Wei, S.Q. Shu, Y. Du, and C. Zhu: Size geometry and nonuniformity effects of surface-nanocrystalline aluminum in nanoindentation test. *Int. J. Plast.* **11,** 2089 (2005).
25. M. Mata and J. Alcala: The role of friction on sharp indentation. *J. Mech. Phys. Solids* **52,** 145 (2004).
26. M. Dao, N. Chollacoop, K.J. Van Vliet, T.A. Venkatesh, and S. Suresh: Computational modelling of the forward and reverse problems in instrumented sharp Indentation. *Acta Mater.* **49,** 3899 (2001).
27. K.K. Tho, S. Swaddiwudhipong, Z.S. Liu, K. Zeng, and J. Hua: Uniqueness of reverse analysis from conical indentation tests. *J. Mater. Res.* **19,** 2498 (2004).
28. J. Alkorta, J.M. Martinez-Esnaola, and J. Gil Sevillana: Absence of one-to-one correspondence between elastoplastic properties and sharp-indentation load-penetration data. *J. Mater. Res.* **20,** 432 (2005).
29. A.C. Fischer-Cripps: *Nonoindentation*, 2nd ed. (Springer Press, New York, 2004).
30. ABAQUS: *Theory Manual Version 6.2* (Hibbitt, Karlsson and Sorensen, Inc., Pawtucket, RI, 2006).
31. S. Jayaraman, G.T. Hahn, W.C. Oliver, and P.C. Bastias: Determination of monotonic stress-strain curve of hard materials from ultra-low-load indentation tests. *Int. J. Solids Struct.* **35,** 365 (1998).
32. M.F. Ashby, D. Cebon, and L. Lee-Shothaman: *Cambridge Engineering Selector V3.1* (Granta Design Limited, Cambridge, 2001).
33. Y.T. Cheng and C.M. Cheng: Can stress-strain relationships be obtained from indentation curves using conical or pyramidal indenters? *J. Mater. Res.* **14,** 3494 (1999).
34. T.W. Capehart and Y.T. Cheng: Determination constitutive models from conical indentation: Sensitivity analysis. *J. Mater. Res.* **18,** 827 (2003).
35. Y.P. Cao and J. Lu: A new method to extract the plastic properties of metal materials from an instrumented spherical indentation loading curve. *Acta Mater.* **52,** 4023 (2004).
36. J.L. Bucaille, S. Stauss, E. Felder, and J. Michler: Determination of plastic properties of metals by instrumented indentation using different sharp indenters. *Acta Mater.* **51,** 1663 (2003).
37. N. Chollacoop, M. Dao, and S. Suresh: Depth-sensing instrumented indentation with dual sharp indenters. *Acta Mater.* **51,** 3713 (2003).
38. Y.P. Cao, X.Q. Qian, J. Lu, and Z.H. Yao: An energy-based method to extract plastic properties of metal materials from conical indentation tests. *J. Mater. Res.* **20,** 1194 (2005).
39. S.Q. Shu and J. Lu: Principles for choosing indenters during the materials properties determined with indentation. *J. Mater. Res.* (2007, to be submitted).
40. Hysitron Incorporated: *Triboscratch User Manual, Software Version 7.0* (Hysitron Inc., Minneapolis, MN, 2001).
41. C.A. Fisher-Cripps and R.L. Brian: Stress analysis of contact

CAMBRIDGE JOURNALS
http://journals.cambridge.org Downloaded: 04 Oct 2013 IP address: 158.132.161.103

deformation in quasi-plastic ceramics. *J. Am. Ceram.Soc.* **19,** 2609 (1996).
42. S.G. Estibaliz: Application of Hertzian tests to measure stress-strain characteristics of ceramics at elevated temperatures. *J. Am. Ceram. Soc.* **90,** 149 (2007).
43. K.T. Kim, S. Cha, and S.Y. Hong: Microstructure and tensile behavior of carbon nanotube reinforced Cu matrix nanocomposites. *Mater. Sci. Eng., A* **430,** 27 (2007).
44. Y.X. Zhou, W. Yang, Y.M. Xia, and P.K. Mallick: An experimental study on the tensile behavior of a unirectional carbon fiber reinforced aluminum composite at different strain rates. *Mater. Sci. Eng., A* **362,** 112 (2003).
45. C.J. Boehlert, B.S. Majumdar, and D.B. Miracle: Application of the cruciform specimen geometry to obtain transverse interface-property data in a high-fiber-volume–fraction SiC/Titanium alloy composite. *Metall. Mater. Trans. A* **32,** 3143 (2001).
46. P. Rupnowski, M. Gentz, and M. Kumosa: Mechanical response of a unidirectional graphite fiber/polyimide composite as a function of temperature. *Compos. Sci. Technol.* **66,** 1045 (2006).

CAMBRIDGE JOURNALS
http://journals.cambridge.org Downloaded: 04 Oct 2013 IP address: 158.132.161.103